

Camphoratsins A–J, Potent Cytotoxic and Anti-inflammatory Triterpenoids from the Fruiting Body of *Taiwanofungus camphoratus*

Shwu-Jen Wu,[†] Yann-Lii Leu,[‡] Chou-Hsiung Chen,[§] Chih-Hua Chao,[§] De-Yang Shen,[§] Hsiu-Hui Chan,[§] E-Jian Lee,[‡] Tian-Shung Wu,^{*,§,▽,+} Yea-Hwey Wang,^{||} Yuh-Chiang Shen,^{||,+} Keduo Qian,[○] Kenneth F. Bastow,[○] and Kuo-Hsiung Lee^{*,▽,○}

Department of Medical Technology, Chung Hua University of Medical Technology, Tainan 717, Taiwan, Republic of China, Natural Products Laboratory, Graduate Institute of Natural Products, Chang Gung University, Kweishan, Taoyuan 333, Taiwan, Republic of China, Department of Chemistry, National Cheng Kung University, Tainan 701, Taiwan, Republic of China, Neurophysiology Laboratory, Neurosurgical Service, Department of Surgery, National Cheng Kung University Medical Center and Medical School, Tainan, Taiwan, Republic of China, College of Pharmacy, China Medical University, Taichung, Taiwan 401, Republic of China, National Research Institute of Chinese Medicine, Taipei 112, Taiwan, Republic of China, Chinese Medicine Research and Development Center, China Medical University and Hospital, Taichung, Taiwan, Republic of China, and Natural Products Research Laboratories, Division of Medicinal Chemistry and Natural Products, UNC Eshelman School of Pharmacy, University of North Carolina, Chapel Hill, North Carolina 27599-7568, United States

Received March 30, 2010

Ten new triterpenoids, camphoratsins A–J (**1–10**), along with 12 known compounds were isolated from the fruiting body of *Taiwanofungus camphoratus*. Their structures were established by spectroscopic analysis and chemical methods. Compound **10** is the first example of a naturally occurring ergosteroid with an unusual *cis*-C/D ring junction. Compounds **2–6** and **11** showed moderate to potent cytotoxicity, with EC₅₀ values ranging from 0.3 to 3 μM against KB and KB-VIN human cancer cell lines. Compounds **6**, **10**, **11**, **14–16**, **18**, and **21** exhibited anti-inflammatory NO-production inhibition activity with IC₅₀ values of less than 5 μM, and were more potent than the nonspecific NOS inhibitor *N*^ω-nitro-L-arginine methyl ester.

Taiwanofungus camphoratus (synonyms: *Ganoderma camphoratum*; *Antrodia cinnamomea*; *Antrodia camphorata*) (Polyporaceae, Aphyllophorales) is a rare and precious medical fungus in Taiwan and is called a “national treasure of Taiwan”.¹ Its Chinese name is Zhan-Ku or Niu-Chang-Chih. The microorganism is parasitic to the inner heartwood wall of old hollow trunks of *Cinnamomum kanehirai* Hay. (Lauraceae). The growth rate of natural *T. camphoratus* in the wild is very slow, and it is difficult to cultivate in a greenhouse, making fruiting bodies expensive to obtain. In traditional Taiwanese folk medicine *T. camphoratus* has been used as an important health food for treating food, alcohol, and drug intoxication, diarrhea, abdominal pain, hypertension, itching, and liver cancer.² Previous studies on the chemical constituents of the fruiting body of *T. camphoratus* showed that it is a rich source of triterpenoidic acids, some of which have shown anti-inflammatory,³ anticholinergic,⁴ and antiserotonergic activities.⁴ Furthermore, zhankuic acids A and C exhibited significant cytotoxicity against P-388 murine leukemia cells in vitro.⁴ The present study on the chemical constituents of an EtOH extract of the fruiting body of *T. camphoratus* has led to the isolation of 10 new triterpenoids, namely, camphoratsins A–J (**1–10**), and 12 known compounds, zhankuic acids A–C (**11–13**),^{4,5} zhankuic acid A methyl ester (**14**),⁴ antcin A (**15**),⁵ antcin C (**16**),⁵ antcin K (**17**),⁶ methyl antcin H (**18**),⁷ eburicol (**19**),⁸ ergosterol D (**20**),⁹ methyl 4 α -methylergost-8,24(28)-diene-3,11-dione-26-oate (**21**),¹⁰ and ergosterol peroxide (**22**).¹¹ Cytotoxic activity, inhibition of nitric oxide (NO) or reactive oxygen species (ROS) production, and free radical-scavenging activity of the isolates were evaluated in our study.

* Corresponding authors. Tel: 919-962-0066. Fax: 919-966-3893. E-mail: khlee@unc.edu; tswu@mail.ncku.edu.tw.

[†] Chung Hua University of Medical Technology.

[‡] Chang Gung University.

[§] Department of Chemistry, National Cheng Kung University.

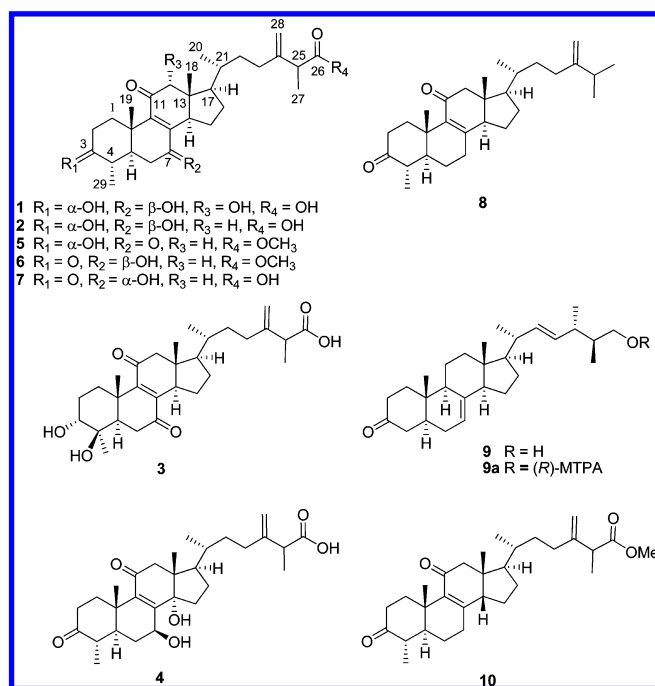
^{||} Neurophysiology Laboratory, National Cheng Kung University Medical Center and Medical School.

[○] National Research Institute of Chinese Medicine.

[▽] China Medical University and Hospital.

⁺ University of North Carolina.

⁺ These authors contributed equally to this work.



Results and Discussion

Camphoratin A (**1**) was obtained as a colorless powder. The HRESIMS of **1** showed a pseudomolecular ion peak at *m/z* 511.3038, consistent with a molecular formula of C₂₉H₄₄O₆Na and eight degrees of unsaturation. The UV and IR absorption bands at 255 nm and 1709, 1660, and 3408 cm⁻¹, respectively, suggested the presence of α,β -unsaturated carbonyl and carboxylic acid functionalities. The former was corroborated by carbon resonances at δ 202.8 (qC), 154.3 (qC), and 141.2 (qC), and the latter was evidenced by the resonance at δ 176.9 (qC). An exocyclic double bond was also identified from the NMR signals at δ _C 150.7 (qC), 110.5 (CH₂) and δ _H 5.07, 5.23 (each 1H, s). The above data, coupled with the characteristic methyl signals at δ _H 0.90 (3H, s), 1.11 (3H, d, *J* = 7.6 Hz), 1.18 (3H, d, *J* = 6.8 Hz), 1.48 (3H, d, *J* = 7.2 Hz),

and 1.57 (3H, s), suggested a 4-methylergost-8-en-11-one skeleton similar to that of antcin C (**16**).⁵ The 3 α -OH functionality was deduced by the correlations from H-3 (δ 3.89, 1H, d, J = 1.6 Hz, β -orientation) to C-4 and C-1 and from H₃-29 to C-3, C-4, and C-5 in the HMBC spectrum of **1**. The hydroxy groups attached at C-7 and C-12 were further designated by the correlations from H-7 (δ 4.52, 1H, t, J = 8.4 Hz) to C-6 and C-8 and from H-12 (4.44, 1H, s) to C-13, C-14, and C-17, respectively. The C-25 carboxylic functionality was assigned due to the presence of an HMBC correlation from H-25 (δ 3.45, 1H, q, J = 6.8 Hz) to the carbon resonance at δ 176.9. A comparison of the NMR spectroscopic data of **1** with those of **16**⁵ confirmed the above elucidation and unambiguously established the structure of **1**. The relative configuration of **1** was determined by the NOE correlations observed in a NOESY experiment. In the NOESY spectrum of **1**, H-7 showed NOE enhancements with both H-5 and H-14, suggesting that these protons had α -orientations. Furthermore, NOE correlations between H-3 and H-4 as well as between H-12 and H₃-18 disclosed that these protons are β -oriented.

Camphoratin B (**2**) was obtained as a colorless syrup. The HRESIMS of **2** gave an $[M + Na]^+$ peak at m/z 495.3089 and established the molecular formula C₂₉H₄₄O₅Na, which is 16 mass units less than that of **1**. The ¹H NMR and ¹³C NMR spectroscopic data of **2** were similar to those of **16** except for the presence of a 3 α -OH in **2** rather than a carbonyl group in **16**. The data were also similar to those of **1** except that the hydroxy-containing methine (C-12) in **1** was replaced by a methylene group in **2**. This assignment was confirmed by the significant upfield shift of H-14 (δ 2.66, 1H, dd, J = 12.0, 6.0 Hz) in **2**, relative to that in **1** (δ 3.57, 1H, dd, J = 12.0, 6.8 Hz), due to the absence of a quasi 1,3-diaxial interaction between H-14 and 12 α -OH. In addition, the HMBC correlations from H₂-12 to C-11, C-13, C-14, and C-18 further supported the above elucidations.

Camphoratin C (**3**) was obtained as a colorless powder and was found to possess the molecular formula C₂₉H₄₂O₆Na, as deduced from the HRESIMS and NMR data. Its IR spectrum showed the presence of hydroxy (3411 cm⁻¹), carboxylic acid (1707 cm⁻¹), and conjugated carbonyl (1674 cm⁻¹) groups. The UV spectrum showed similar absorption bands to those of **11**–**13**,⁴ which indicated the presence of an 8(9)-ene-7,11-dione moiety. This assignment was further corroborated by the carbon resonances at δ 203.05 (qC), 203.0 (qC), 155.0 (qC), and 144.2 (qC). A comparison of NMR spectroscopic data of **3** with those of **17**⁶ revealed identical substitution at C-3 and C-4, while the C-7 hydroxy group in **17** was oxidized to a carbonyl moiety in **3**.

Camphoratin D (**4**) was isolated as a colorless powder and exhibited an $[M + Na]^+$ peak at m/z 509.2875, corresponding to a molecular formula of C₂₉H₄₂O₆Na as obtained from HRESIMS. Its IR spectrum showed the presence of hydroxy (3444 cm⁻¹), carbonyl (1708 cm⁻¹), and conjugated ketone (1674 cm⁻¹) groups. The UV spectrum showed absorption bands at 246 nm, suggesting the presence of an 8(9)-en-11-one moiety,⁵ which was corroborated by the carbon resonances at δ 199.5 (qC), 154.3 (qC), and 141.2 (qC). The proton resonance at δ 4.98 (1H, t, J = 8.4 Hz) was attributed to the 7 β -hydroxy functionality. The other carbonyl carbon resonance at δ 211.0 was assigned to C-3 due to the observation of HMBC correlations from H₃-29 to C-3, C-4, and C-5. The side-chain moiety was found to be the same as that in **1**–**3**. Moreover, a hydroxy-containing quaternary carbon was assigned at C-14 according to the downfield shift of C-15 as compared to the corresponding carbon in **1**–**3**. In the ¹³C NMR spectrum of **4**, the significant upfield shift for C-12 (Δ = -9.4 ppm) and C-17 (Δ = -5.5 ppm) as well as the downfield shift for C-18 (Δ = +3.9 ppm), relative to those in **2** (C-12, δ 58.9; C-17, δ 55.0), suggested an α -orientation for 14-OH.^{7,12}

Camphoratin E (**5**), a colorless syrup, was found to possess the molecular formula C₃₀H₄₄O₅, as deduced from the HRESIMS and

NMR spectroscopic data. Its IR spectrum showed the presence of hydroxy (3491 cm⁻¹), ester (1730 cm⁻¹), and conjugated carbonyl (1678 cm⁻¹) groups. The UV absorption band at ν_{\max} 260 nm and carbon resonances at δ 203.1 (qC), 202.1 (qC), 153.7 (qC), and 144.7 (qC) indicated the presence of an 8(9)-ene-7,11-dione moiety. The NMR spectroscopic data of **5** were similar to those of **12**⁴ except for additional methoxy signals at δ_{H} 3.66 and δ_{C} 51.9, which suggested that **5** is the methyl ester of **12**. In the ¹³C NMR spectra of **5**, several smaller signals at δ_{C} 31.0, 45.5, and 16.3 revealed the presence of an epimeric mixture at C-25.⁴

The HRESIMS of camphoratin F (**6**) established the same molecular formula, C₃₀H₄₄O₅, as that of **5**. Its UV and IR spectra showed the presence of an 8(9)-en-11-one moiety (λ_{\max} 251 nm and ν_{\max} 1669 cm⁻¹), a carbonyl group (1711 cm⁻¹), and an ester moiety (1735 cm⁻¹). Comparison of the NMR data of **6** and **5** showed that the hydroxy-linked methine resonance of H-3 in **5** was absent from the NMR spectrum of **6** and was replaced by a carbonyl functionality at δ_{C} 212.3. In addition, the carbon resonance for the C-7 carbonyl group in **5** was converted to a hydroxy-linked methine (δ_{H} 4.39, 1H, t, J = 8.0 Hz) in **6**. A β -orientation of the hydroxy group at C-7 was deduced by the splitting pattern of H-7 as compared to those in **1** and **2**. Similarly to **5**, the NMR data of **6** showed the presence of an epimeric mixture at C-25 (Table 1).

Camphoratin G (**7**) was found to have the molecular formula C₂₉H₄₂O₅, 14 mass units less than **6**, as deduced from the HRESIMS and NMR data. The UV and IR spectra of **7** were similar to those of **6**, except that a carboxylic acid moiety was observed in **7** (ν_{\max} 1707 cm⁻¹) rather than an ester group. Consequently, the structure of **7** might be structurally related to **6**. Comparison of ¹H NMR data of **7** with those of **6**, antcin F, and methyl antcin G⁷ disclosed that **7** might be a C-7 epimer of antcin F. Moreover, the splitting pattern of H-7 (d, J = 2.0 Hz) in **7** suggested a β -oriented proton⁷ rather than an α -proton like those in **1**, **2**, and **6**.

The HRESIMS of camphoratin H (**8**) gave a pseudomolecular ion peak at m/z 447.3237 $[M + Na]^+$, corresponding to the molecular formula C₂₉H₄₄O₂Na. Its UV and IR spectra showed the presence of an 8(9)-en-11-one moiety (λ_{\max} 248 nm and ν_{\max} 1678 cm⁻¹) and a carbonyl group (1711 cm⁻¹). Its ¹H NMR spectrum displayed signals for six methyl groups at δ_{H} 0.74 (s), 0.95 (d), 1.03 (d), 1.06 (d), 1.29 (d), and 1.34 (s). The above data coupled with the absence of the carbon resonance appropriate for a carboxylic acid or a methyl ester moiety suggested that **8** possesses a 4-methylergost-8-en-11-one skeleton. The NMR spectra of **8** were similar to those of **15**,⁵ except that the NMR signals appropriate for a carboxylic functionality were replaced by signals for a C-25 methyl group.

Camphoratin I (**9**) was found to have the molecular formula C₂₈H₄₄O₂ from HRESIMS analysis. The absence of UV absorption bands from 240 to 270 nm disclosed that **9** did not possess an 8(9)-ene-7,11-dione or 8(9)-en-11-one moiety. The IR and ¹³C NMR data of **9** showed the presence of 28 carbon signals, including one carbonyl group (δ 211.9, ν_{\max} 1716 cm⁻¹), two double bonds (δ 139.4, 117.1, 136.7, and 130.4), and one hydroxymethyl moiety (δ 66.9, ν_{\max} 3336 cm⁻¹). The above data, coupled with the characteristic methyl signals at δ_{H} 0.57 (3H, s), 0.86 (3H, d, J = 6.8 Hz), 1.00 (3H, d, J = 6.8 Hz), 1.01 (3H, s), and 1.02 (3H, d, J = 7.2 Hz), suggested that **9** is similar to the known compound ergost-7-en-3-one.¹³ By comparison of the ¹³C NMR spectroscopic data of **9** with those of ergost-7-en-3-one, it was found that resonances for the nucleus of both compounds were superimposable, revealing that they have different substitution patterns in the side-chain moiety. This was confirmed by the HMBC correlations from H₃-21 to C-17, C-20, and C-22, from H₃-28 to C-23, C-24, and C-25, and from H₃-27 to C-24, C-25, and C-26. Comparison of the NMR data of C-24, C-27, and C-28 of **9** with those of synthetic compounds led to the establishment of an *erythro* configuration at C-24 and C-25 (24*S*,25*S* or 24*R*,25*R*). Furthermore, the 24*S*,25*S*

Table 1. ^{13}C NMR Data for Compounds **1–4** (in pyridine- d_5) and **5–10** (in CDCl_3)

| position | 1 ^a | 2 ^a | 3 ^a | 4 ^b | 5 ^a | 6 ^a | 7 ^b | 8 ^a | 9 ^a | 10 ^a |
|----------|----------------|----------------|----------------|----------------|----------------|----------------|----------------|----------------|----------------|-----------------|
| 1 | 29.7 | 29.8 | 28.8 | 36.3 | 27.8 | 35.7 | 34.6 | 35.5 | 38.8 | 35.1 |
| 2 | 30.6 | 30.7 | 26.6 | 38.0 | 29.1 | 37.8 | 37.5 | 37.0 | 38.1 | 37.8 |
| 3 | 70.3 | 70.2 | 74.3 | 211.0 | 70.3 | 212.3 | 212.8 | 213.7 | 211.9 | 213.1 |
| 4 | 35.0 | 35.4 | 74.0 | 43.8 | 34.5 | 43.8 | 43.8 | 44.8 | 44.2 | 44.3 |
| 5 | 40.4 | 40.4 | 44.6 | 47.7 | 41.1 | 48.2 | 44.6 | 51.0 | 42.9 | 50.6 |
| 6 | 32.9 | 32.7 | 37.0 | 35.0 | 38.1 | 32.5 | 31.3 | 21.3 | 30.0 | 21.1 |
| 7 | 70.1 | 70.1 | 203.5 | 70.5 | 202.1 | 69.9 | 70.2 | 30.6 | 117.1 | 32.3 |
| 8 | 154.3 | 155.1 | 155.0 | 154.3 | 144.7 | 153.2 | 153.0 | 157.5 | 139.4 | 154.6 |
| 9 | 141.2 | 143.0 | 144.2 | 141.2 | 153.7 | 141.2 | 140.7 | 139.1 | 48.9 | 138.0 |
| 10 | 37.7 | 38.1 | 40.4 | 38.5 | 38.7 | 37.0 | 37.2 | 38.2 | 34.4 | 36.4 |
| 11 | 202.8 | 201.8 | 203.0 | 199.5 | 203.1 | 201.3 | 200.9 | 200.3 | 21.7 | 200.4 |
| 12 | 81.7 | 58.9 | 58.0 | 49.5 | 57.5 | 57.9 | 57.6 | 58.1 | 39.3 | 53.2 |
| 13 | 50.7 | 48.2 | 47.7 | 47.5 | 47.3 | 47.6 | 47.1 | 47.6 | 43.3 | 44.0 |
| 14 | 47.3 | 53.9 | 49.9 | 83.2 | 49.5 | 53.0 | 51.2 | 53.5 | 55.0 | 55.3 |
| 15 | 25.4 | 25.6 | 25.7 | 32.1 | 24.9 | 24.8 | 23.1 | 24.1 | 22.9 | 29.3 |
| 16 | 27.8 | 28.4 | 28.2 | 26.2 | 27.8 | 27.8 | 27.5 | 28.0 | 28.1 | 30.4 |
| 17 | 46.0 | 55.0 | 54.3 | 49.5 | 53.9 | 54.4 | 55.1 | 55.8 | 55.8 | 55.8 |
| 18 | 12.4 | 12.7 | 12.3 | 16.6 | 11.9 | 12.1 | 12.2 | 12.1 | 12.1 | 22.3 |
| 19 | 18.3 | 17.1 | 19.7 | 17.1 | 15.9 | 17.5 | 16.3 | 17.8 | 12.4 | 18.0 |
| 20 | 36.5 | 36.4 | 36.1 | 35.7 | 35.7 | 35.7 | 35.8 | 36.3 | 40.5 | 33.3 |
| 21 | 18.3 | 18.8 | 18.8 | 19.4 | 18.5 | 18.5 | 18.4 | 18.8 | 21.1 | 19.5 |
| 22 | 34.9 | 34.7 | 34.6 | 34.0 | 33.8 | 33.9 | 33.8 | 34.8 | 136.7 | 32.8 |
| 23 | 32.1 | 31.9 | 31.9 | 32.1 | 31.2 | 31.2 | 30.7 | 31.3 | 130.4 | 31.9 |
| 24 | 150.7 | 150.6 | 150.6 | 150.2 | 148.5 | 148.4 | 148.1 | 156.9 | 38.1 | 148.5 |
| 25 | 46.8 | 46.9 | 46.9 | 46.7 | 45.7 | 45.7 | 45.1 | 34.3 | 40.8 | 45.7 |
| 26 | 176.9 | 177.0 | 177.0 | 176.7 | 175.0 | 175.0 | 177.4 | 22.2 | 66.9 | 175.0 |
| 27 | 17.3 | 17.2 | 17.3 | 17.2 | 16.4 | 16.4 | 16.2 | 22.3 | 12.7 | 16.4 |
| 28 | 110.5 | 110.7 | 110.7 | 110.5 | 110.9 | 110.9 | 111.5 | 106.6 | 18.3 | 110.9 |
| 29 | 17.1 | 17.1 | 27.5 | 12.0 | 15.7 | 11.5 | 11.9 | 12.2 | | 11.6 |
| OMe | | | | | 51.9 | 51.9 | | | | 51.9 |

^a Recorded at 100 MHz at 25 °C. ^b Recorded at 125 MHz at 25 °C. ^c Chemical shifts for 25-epimer.

configuration for **9** was confirmed by the preparation of its (*R*)-MTPA ester, in which the proton resonance of H₂-26 showed a broad doublet at δ 4.17.¹⁴ In addition, the MTPA ester helped to establish the *E* geometry of the C-22–C-23 double bond by a 15.0 Hz coupling constant.

The molecular formula of camphoratin J (**10**) was assigned as C₃₀H₄₄O₄ on the basis of its HRESIMS. Its UV and IR spectra showed the presence of an 8(9)-en-11-one moiety (λ_{max} 250 nm and ν_{max} 1669 cm⁻¹), a carbonyl group (1709 cm⁻¹), and an ester moiety (1738 cm⁻¹). The 8(9)-en-11-one moiety was deduced by the carbon resonances at δ 200.4, 138.0, and 154.6 and HMBC correlations from H₂-12 to the carbonyl carbon. The carbonyl and methyl ester functionalities were assigned at C-3 and C-25, respectively, on the basis of the HMBC correlations from H₃-29 to C-3, C-4, and C-5 and from H-25 to the carbon resonance at δ 175.0, which was also correlated with the methoxy group at δ_{H} 3.66 (3H, s). The inspection of the 2D NMR spectra led to the establishment of the same planar structure as the known compound methyl 4 α -methylergost-8,24(28)-diene-3,11-dion-26-oate.¹⁰ However, both compounds differed in carbon resonances for rings C and D, revealing the presence of epimers at the C/D ring junction. The relative configuration of the C/D ring junction in **10** was elucidated by the NOE enhancements observed in a selective 1D NOESY experiment. Irradiation of H₃-18 caused enhancements of H-14, H-20, and H₃-21, but not of H-17, suggesting a *cis*-fused C/D ring. The downfield shift ($\Delta = +10.4$ ppm) of C-18 in the ^{13}C NMR spectrum of **10**, relative to that observed for methyl 4 α -methylergost-8,24(28)-diene-3,11-dion-26-oate, was also in agreement with a rare *cis* C/D ring junction, which has been found in compounds from marine sponges.^{15–17} Additional smaller carbon signals at δ_{C} 31.8, 45.5, and 16.3 were attributed to the other C-25 epimer. Compound **10** represents the first ergosteroid with a *cis*-fused C/D ring junction.

The cytotoxicity of the new and known compounds (**1–19**) was evaluated in parallel with etoposide against the human cancer cell

line KB and multi-drug-resistant strain KB-VIN in vitro (Table 4). Several of the compounds, including **2–7**, **11–13**, and **15**, showed moderate to potent cytotoxic activity, with EC₅₀ values ranging from 0.3 to 15.5 μM . Compounds **3** and **5** showed the highest cytotoxicity against the KB cell line, with EC₅₀ values of 0.3 and 0.45 μM , respectively. Compounds **4** and **6** also showed cytotoxicity against KB, with EC₅₀ values of 1.0 and 2.0 μM , respectively. More importantly, compounds **4** and **6** retained their activity against multiresistant strain KB-VIN, with EC₅₀ values of 1.4 and 2.9 μM , respectively. It appeared that **4** and **6** were not substrates of P-glycoprotein (P-gp), a key transporter related to drug resistance, based on the lack of cross-resistance shown by KB-VIN. By comparison, etoposide, a known P-gp substrate, was at least 8-fold less active in the KB-VIN cell line. Comparing the structures of compounds **3–6**, we find that **3** and **5** contain the same C-3 α -hydroxy group and C-7 keto moiety, while **4** and **6** contain a C-3 keto and C-7 β -hydroxy group. It seems that the latter triterpene scaffold may overcome the resistance issue. Compound **3** has an additional C-4 β -hydroxy group and a free carboxylic acid tail in its R₅ moiety, which may contribute to the best activity profile of the series.

The anti-inflammatory activities of **2**, **6**, and **9–22** were evaluated by examining their effects on lipopolysaccharide (LPS)-induced inducible-nitric oxide synthase (iNOS)-dependent NO production and NADPH oxidase (NOX)-dependent ROS production in murine microglial cells (BV2) and peripheral human neutrophils (PMN). Compounds **6**, **10**, **11**, **14–16**, **18**, and **21** significantly inhibited NOS activity, with IC₅₀ values of 2.5, 1.6, 3.6, 0.6, 4.1, 4.2, 2.5, and 1.5 μM , respectively. They were more potent than N^w-nitro-L-arginine methyl ester (L-NAME) (IC₅₀ 25.8 μM), a nonspecific NOS inhibitor, at inhibiting LPS-induced NO production (Table 5). The remaining compounds, except for **20**, inhibited NOS activity with IC₅₀ values ranging from 6.3 to 22.3 μM (Table 5). NOX is the major ROS-producing enzyme in activated inflammatory cells.¹⁸ We previously reported that drugs with anti-inflammatory activity

Table 2. ¹H NMR Data for Compounds **1–4** (in Pyridine-*d*₅)

| position | 1 ^a | 2 ^a | 3 ^a | 4 ^b |
|----------|---------------------------|--------------------------------|--|--------------------------------|
| 1 | 1.93 m 2.78 m | 1.85 m 2.85 m | 2.10 td (13.2, 3.2) 3.04 dt (13.2, 3.2) | 1.50 m 3.28 m |
| 2 | 1.86 m 1.93 m | 1.86 m 1.89 m | 1.92 m 2.74 m | 2.40 m 2.52 m |
| 3 | 3.89 d (1.6) ^c | 3.91 d (2.4) | 4.02 br s | |
| 4 | 1.64 m | 1.62 m | | 2.39 m |
| 5 | 2.13 m | 2.02 m | 2.65 m | 1.50 m |
| 6 | 1.74 m 2.42 m | 1.67 m 2.39 m | 2.90 dd (13.2, 3.2) 3.14 t (13.2) | 2.23 m 2.51 m |
| 7 | 4.52 t (8.4) | 4.50 t (8.4) | | 4.98 t (8.4) |
| 12 | 4.44 s | 2.43 d (13.2) 2.95 d (13.2) | 2.46 d (13.2) 2.97 d (13.2) | 2.74 d (15.8) 2.89 d (15.8) |
| 14 | 3.57 dd (12.0, 6.8) | 2.66 dd (12.0, 6.0) | 2.67 m | |
| 15 | 2.19 m 2.50 m | 2.01 m 2.49 m | 1.66 m 2.74 m | 1.80 m |
| 16 | 1.42 m | 1.45 | 1.44 | 1.60 m 1.83 m |
| 17 | 2.42 m | 1.43 m | 1.42 m | 1.75 m |
| 18 | 0.90 s | 0.88 s | 0.72 s | 1.22 s |
| 19 | 1.57 s | 1.49 s | 1.99 s | 1.45 s |
| 20 | 1.41 m | 1.40 m | 1.38 | 1.56 m |
| 21 | 1.11 d (7.6) | 0.89 d (7.6) | 0.87 d (5.2) | 1.01 d (6.5) |
| 22 | 1.37 m 1.81 m | 1.31 m 1.75 m | 1.30 m 1.75 m | 1.27 m 1.88 m |
| 23 | 2.25 m 2.44 m | 2.20 m 2.39 m | 2.20 m 2.38 m | 2.23 m 2.42 m |
| 25 | 3.45 q (6.8) | 3.45 q (7.2) | 3.45 q (7.2) | 3.44 q (7.2) |
| 27 | 1.48 d (7.2) | 1.49 d (6.8) | 1.49 d (7.2) | 1.47 d (7.2) |
| 28 | 5.07 s 5.23 s | 5.06 s 5.22 s | 5.06 s 5.23 s | 5.06 s 5.21 s |
| 29 | 1.18 d (6.8) | 1.18 d (6.4) | 1.61 s | 1.11 d (6.6) |

^a Recorded at 400 MHz at 25 °C. ^b Recorded at 500 MHz at 25 °C. ^c *J* values (in Hz) in parentheses.

also show potent NOX-inhibitory action.^{19,20} Therefore, we evaluated the isolates for effects on NOX activity in lysates of microglial cells and PMN. Our data suggest that none of the tested compounds were potent inhibitors of NOX in lysates of microglial cells and PMN, relative to the specific NOX inhibitor diphenyleioidonium (DPI) (IC₅₀ 0.4 and 0.3 μM, respectively) (Table 5). In addition, the free radical-scavenging capacities of these compounds were examined in a cell-free 1,1-diphenyl-2-picrylhydrazyl (DPPH) solution. None of the tested compounds showed significant free radical-scavenging activity.

Although it is now clear that proliferation of cells alone does not cause cancer, sustained cell proliferation in an environment rich in inflammatory cells, growth factors, activated stroma, and DNA-damage-promoting agents certainly potentiates and/or promotes neoplastic risk.²¹ In many circumstances, inflammation orchestrates the microenvironment around tumors, contributing to proliferation, survival, and migration. Cancer cells also use selectins, chemokines, and their receptors (involved in inflammatory response) for invasion, migration, and metastasis. Interestingly, Peng et al. found that a crude extract of *Antrodia camphorata* (*Taiwanofungus camphoratus*) significantly inhibited proliferation of three transitional cell carcinoma (TCC) cell lines (RT4, a superficial cancer cell line, and TSGH-8301 and T24, two metastatic cancer cell lines), likely through different mechanisms.²² Combined with our observations in this study, it would be interesting to evaluate whether the antitumor invasion effect in the crude extract could be mediated through the anti-inflammatory properties of the contained triterpenoids. Thus, the newly identified camphoratin analogues with both potent cytotoxicity and anti-inflammatory activity merit further investigation as cancer chemotherapeutic agents or as anti-inflammatory drugs for the treatment of NO-dependent neurodegenerative disorders.

Experimental Section

General Experimental Procedures. Melting points were determined on a Yanagimoto MP-S3 micromelting point apparatus. IR spectra were recorded on a Shimadzu Prestige-21 FTIR spectrometer. Optical rotations

were measured using a Jasco DIP-370 polarimeter. UV spectra were obtained on a Hitachi UV-3210 spectrophotometer. ESI and HRESI mass spectra were recorded on a Bruker APEX II mass spectrometer. The NMR spectra, including ¹H NMR, ¹³C NMR, COSY, NOESY, HMBC, and HMQC experiments, were recorded on Bruker AVANCE-500 and AMX-400. Silica gel (E. Merck 70–230, 230–400 mesh) was used for column chromatography.

Fungal Material. Wild fruiting bodies of *T. camphoratus*, which were grown in Ping-Tung County, Taiwan, were purchased from the Kaohsiung Society for Wildlife and Nature in 2003. The fungus was identified by Dr. Tun-Tschu Chang (Taiwan Forestry Research Institute). A voucher specimen (TSWu 2003005) was deposited in the Department of Chemistry, National Cheng Kung University, Tainan, Taiwan.

Extraction and Isolation. The fruiting body of *T. camphoratus* (1.0 kg) was extracted with EtOH (4 × 10 L) under reflux for 8 h. The EtOH extract was concentrated to afford a brown syrup (161 g) and then partitioned between H₂O and *n*-hexane. The *n*-hexane layer (9.3 g) was chromatographed on silica gel and eluted with EtOAc in *n*-hexane (0–100% of EtOAc, gradient) to obtain 10 fractions. Fraction 4 was rechromatographed on a silica gel column using *n*-hexane–Me₂CO (19:1) as eluent to yield **8** (3.0 mg), **9** (6.0 mg), **10** (4.5 mg), **19** (22.0 mg), **20** (90.2 mg), **21** (22.1 mg), and **22** (16.5 mg). Compound **22** (41.1 mg) was obtained in the same way from fraction 8. The water layer (145 g) was filtered and concentrated under reduced pressure to give a brown syrup (55 g) and a water-insoluble portion (89 g). The water-insoluble portion was chromatographed on a silica gel column using CHCl₃–MeOH mixtures of increasing polarity for elution to obtain 10 fractions (WI-1–WI-10). Compounds **1** (2.2 mg), **5** (2.0 mg), **6** (14.2 mg), **9** (1.0 mg), **14** (1.29 g), **15** (53.8 mg), and **21** (62.2 mg) were obtained from a combined fraction (fractions WI-1 and WI-2) by silica gel column chromatography with gradient elution (CHCl₃–Me₂CO, 39:1 to 14:1). Fraction WI-3 was separated on a silica gel column using *i*-Pr₂O–MeOH (19:1) as the eluent to yield **11** (141.5 mg), **18** (11.0 mg), **16** (122.9 mg), and **12** (53.0 mg). Fraction WI-4 was chromatographed on a silica gel column with *i*-Pr₂O–MeOH (12:1) to give **7** (11.3 mg), **18** (38.0 mg), **16** (708.0 mg), and **12** (66.5 mg). Compounds **2** (5.0 mg), **4** (2.2 mg), **7** (3.4 mg), and **13** (286.2 mg) were obtained from fraction WI-5 using silica gel column

Table 3. ¹H NMR Data for Compounds **5–10** (in CDCl₃)

| position | 5 ^a | 6 ^a | 7 ^b | 8 ^a | 9 ^a | 10 ^a |
|----------|-----------------------------|-----------------------------|----------------|-------------------------------------|---------------------|-----------------|
| 1 | 1.40 m | 1.25 m | 1.26 m | 1.33 m | 1.49 m | 1.33 m |
| | 2.50 m | 2.95 m | 2.95 m | 3.18 m | 2.13 m | 2.88 m |
| 2 | 1.72 m | 2.35 m | 2.40 m | 2.35 m | 2.30 m | 2.37 m |
| | 1.94 m | 2.49 m | 2.49 m | 2.51 m | 2.42 td (14.4, 8.8) | 2.50 m |
| 3 | 3.79 br s | | | | | |
| 4 | 1.74 m | 2.35 m | 2.40 m | 2.36 m | 2.24 m | 2.38 m |
| 5 | 2.12 m | 1.39 m | 1.46 m | 1.39 m | 1.83 m | 1.41 m |
| 6 | 2.25 t (15.1) ^c | 1.56 m | 1.57 m | 1.43 m | 1.27 m | 1.42 m |
| | 2.41 dd (15.1, 3.0) | 2.49 m | 1.89 m | 1.78 m | 1.83 m | 1.78 m |
| 7 | | 4.39 t (8.0) | 4.26 d (2.0) | 2.18 m | 5.18 br s | 2.11 m |
| | | | | 2.37 m | | 2.30 m |
| 9 | | | | | 1.75 m | |
| 11 | | | | | 1.54 m | |
| | | | | | 1.64 m | |
| 12 | 2.40 d (13.6) | 2.32 d (14.0) | 2.38 d (14.5) | 2.33 d (14.4) | 1.27 m | 2.18 d (13.9) |
| | 2.89 d (13.6) | 2.83 d (14.0) | 2.84 d (14.5) | 2.80 d (14.4) | 2.04 m | 2.47 d (13.9) |
| 14 | 2.62 dd (12.4, 7.0) | 2.71 m | 2.78 m | 2.64 dd (12.0, 7.6) | 1.81 m | 2.09 m |
| 15 | 1.47 m | 1.90 m | 1.90 m | 1.52 m | 1.41 m | 1.37 m |
| | 2.55 m | 2.09 m | 2.07 m | 1.81 m | 1.52 m | 1.93 m |
| 16 | 1.25 m | 1.44 m | 1.40 m | 1.42 m | 1.29 m | 1.47 m |
| | 1.98 m | 1.96 m | 1.90 m | 1.81 m | 1.73 m | 2.08 m |
| 17 | 1.42 m | 1.38 m | 1.46 m | 1.48 m | 1.28 m | 1.39 m |
| 18 | 0.67 s | 0.77 s | 0.72 s | 0.74 s | 0.57 s | 1.02 s |
| 19 | 1.31 s | 1.44 s | 1.26 s | 1.34 s | 1.01 s | 1.37 s |
| 20 | 1.42 m | 1.41 m | 1.43 m | 1.47 m | 2.05 m | 1.46 m |
| 21 | 0.93 d (5.6) | 0.92 d (5.5) | 0.93 d (6.0) | 0.95 d (5.6) | 1.02 d (7.2) | 0.90 d (6.4) |
| 22 | 1.18 m | 1.25 m | 1.32 m | 1.22 m | 5.25 m | 1.17 m |
| | 1.57 m | 1.58 m | 1.59 m | 1.53 m | | 1.47 m |
| 23 | 1.95 m | 1.98 m | 2.00 m | 1.89 m | 5.25 m | 1.95 m |
| | 2.16 m | 2.15 m | 2.17 m | 2.10 m | | 2.14 m |
| 24 | | | | | 2.23 m | |
| 25 | 3.13 q (7.0) | 3.12 q (6.8) | 3.16 q (7.0) | 2.24 m | 1.58 m | 3.13 q (7.0) |
| 26 | | | | 1.06 d (6.8) | 3.45 dd (10.4, 6.4) | |
| | | | | | 3.56 dd (10.4, 6.4) | |
| 27 | 1.28 d (7.0) | 1.27 d (6.8) | 1.30 d (7.5) | 1.03 d (6.8) | 0.86 d (6.8) | 1.28 d (7.0) |
| 28 | 4.92 s, 4.88 s | 4.91 s, 4.89 s | 4.94 s | 4.67 s | 1.00 d (6.8) | 4.92 s, 4.88 s |
| | 4.90 s, 4.86 s ^d | 4.87 s, 4.85 s ^d | 4.99 s | 4.74 s, 4.90 s, 4.87 s ^d | | |
| 29 | 0.96 d (6.4) | | 1.03 d (7.0) | 1.29 d (6.8) | | 1.04 d (6.6) |
| OMe | 3.66 s | 3.66 s | | | | 3.66 s |

^a Recorded at 400 MHz at 25 °C. ^b Recorded at 500 MHz at 25 °C. ^c *J* values (in Hz) in parentheses. ^d Chemical shifts for 25-epimer.

Table 4. In Vitro Cytotoxicity of Compounds **1–19**

| compd | EC ₅₀ (μM) | |
|-----------|-----------------------|----------|
| | KB | KB-VIN |
| 1 | NA ^a | NA |
| 2 | 1.8 | NA |
| 3 | 0.3 | 2.3 |
| 4 | 1.0 | 1.4 |
| 5 | 0.45 | 2.7 |
| 6 | 2.0 | 2.9 |
| 7 | 15.0 | 17.5 |
| 8 | NA | NA |
| 9 | NA | NA |
| 10 | NA | NA |
| 11 | 3.0 | 6.2 |
| 12 | 7.3 | 8.5 |
| 13 | 15.5 | 6.4 |
| 14 | >20 (21) ^b | >20 (25) |
| 15 | 4.9 | 10.0 |
| 16 | NA | NA |
| 17 | NA | NA |
| 18 | NA | NA |
| 19 | >20 (34) | >20 (18) |
| etoposide | 4.5 | >36 |

^a NA: not active. No growth inhibition at 20 μM. ^b Values in parentheses are % inhibition at 20 μM.

chromatography (eluent, CHCl₃–MeOH, 12:1). Fractions WI-6 and WI-7 were combined and rechromatographed on a silica gel column with CHCl₃–MeOH (6:1) as the mobile phase to afford **3** (3.8 mg) and **13** (1.81 g). Compound **17** (1.16 g) was isolated from a combined fraction (fractions WI-8 and WI-9) by silica gel column chromatography using *i*-Pr₂O–MeOH (4:1) as the eluent.

Camphoratin A (3α,7β,11α-trihydroxy-11-oxo-4α-methylergosta-8,24(28)-dien-26-oic acid, 1): colorless powder (MeOH); mp 117–119 °C; [α]_D²⁵ +221 (*c* 0.001, MeOH); UV (MeOH) λ_{max} (log ε) 255 (3.49) nm; IR (KBr) ν_{max} 3408, 2959, 2930, 2875, 1709, 1660, 1215, 1059 cm⁻¹; ¹H NMR and ¹³C NMR, see Tables 1 and 2; ESIMS *m/z* 511 [M + Na]⁺; HRESIMS *m/z* 511.3038 (calcd for C₂₉H₄₄O₆Na 511.3035).

Camphoratin B (3α,7β-dihydroxy-11-oxo-4α-methylergosta-8,24(28)-dien-26-oic acid, 2): colorless syrup; [α]_D²⁵ +54 (*c* 0.006, MeOH); UV (MeOH) λ_{max} (log ε) 255 (3.79) nm; IR (KBr) ν_{max} 3420, 2962, 2935, 2878, 1709, 1659, 1217, 1083 cm⁻¹; ¹H NMR and ¹³C NMR, see Tables 1 and 2; ESIMS *m/z* 495 [M + Na]⁺; HRESIMS *m/z* 495.3089 (calcd for C₂₉H₄₄O₅Na 495.3086).

Camphoratin C (3α,4β-dihydroxy-7,11-dioxo-4α-methylergosta-8,24(28)-dien-26-oic acid, 3): colorless powder (MeOH); mp 186–188 °C; [α]_D²⁵ +57 (*c* 0.067, MeOH); UV (MeOH) λ_{max} (log ε) 271 (3.80) nm; IR (KBr) ν_{max} 3411, 2966, 2936, 2878, 1709, 1674, 1230, 1062 cm⁻¹; ¹H NMR and ¹³C NMR, see Tables 1 and 2; ESIMS *m/z* 509 [M + Na]⁺; HRESIMS *m/z* 509.2874 (calcd for C₂₉H₄₂O₆Na 509.2879).

Camphoratin D (7β,14α-dihydroxy-3,11-dioxo-4α-methylergosta-8,24(28)-dien-26-oic acid, 4): colorless powder (MeOH); mp 175–177 °C; [α]_D²⁵ +34 (*c* 0.004 MeOH); UV (MeOH) λ_{max} (log ε) 246 (3.97) nm; IR (KBr) ν_{max} 3444, 2971, 2936, 2878, 1708, 1670, 1229, 1187, 1068, cm⁻¹; ¹H NMR and ¹³C NMR, see Tables 1 and 3; ESIMS *m/z* 509 [M + Na]⁺; HRESIMS *m/z* 509.2875 (calcd for C₂₉H₄₂O₆Na 509.2879).

Camphoratin E (methyl 3α-hydroxy-7,11-dioxo-4α-methylergosta-8,24(28)-dien-26-oate, 5): colorless syrup; [α]_D²⁵ +166 (*c* 0.007, MeOH); UV (MeOH) λ_{max} (log ε) 260 (3.68) nm; IR (KBr) ν_{max} 3491, 2959, 2936, 2877, 1730, 1678, 1235, 1202, 1169 cm⁻¹; ¹H NMR and ¹³C NMR, see Tables 1 and 3; ESIMS *m/z* 507 [M + Na]⁺; HRESIMS *m/z* 507.3088 (calcd for C₃₀H₄₄O₅Na 507.3086).

Table 5. Effects of Compounds **2**, **6**, and **9–22** on NOX Activity^a in Murine Microglial Cells and PMN and on NOS Activity^b in Murine Microglial Cells

| compound | IC ₅₀ (μM) in NOX | | IC ₅₀ (μM) in NOS |
|-----------|-------------------------------|------------------------------------|------------------------------|
| | activity from BV2 cell lysate | fMLP-induced NOX activation in PMN | |
| 2 | NA | 32.1 ± 3.5 ^c | 15.7 ± 0.9 ^c |
| 6 | NA | 11.2 ± 2.3 ^c | 2.5 ± 0.6 ^c |
| 9 | NA | 17.5 ± 3.9 ^c | 12.7 ± 2.2 ^c |
| 10 | NA | 15.8 ± 4.0 ^c | 1.6 ± 0.6 ^c |
| 11 | NA | 22.1 ± 6.7 ^c | 3.6 ± 0.8 ^c |
| 12 | NA | NA | 9.6 ± 0.7 ^c |
| 13 | 40.3 ± 3.5 ^c | NA | 16.2 ± 0.9 ^c |
| 14 | NA | 8.4 ± 2.1 ^c | 0.6 ± 0.3 ^c |
| 15 | 45.9 ± 7.9 ^c | 29.2 ± 6.7 ^c | 4.1 ± 0.5 ^c |
| 16 | NA | 22.6 ± 3.3 ^c | 4.2 ± 1.2 ^c |
| 17 | NA | 47.2 ± 8.4 ^c | NA |
| 18 | 16.0 ± 8.1 ^c | 18.1 ± 5.9 ^c | 2.5 ± 0.3 ^c |
| 19 | NA | 21.9 ± 6.3 ^c | 22.3 ± 2.9 ^c |
| 20 | NA | 27.9 ± 5.6 ^c | 30.6 ± 0.8 ^c |
| 21 | NA | 16.2 ± 4.3 ^c | 1.5 ± 0.7 ^c |
| 22 | NA | 20.3 ± 6.4 ^c | 6.3 ± 1.8 ^c |
| DPI | 0.4 ± 0.2 | 0.3 ± 0.1 | — |
| L-NAME | — | — | 25.8 ± 2.5 |

^a NOX activity was measured as ROS production triggered with NADPH (200 μM) or fMLP (2 μM) in the presence of 1–50 μM of test drugs in BV2 cell lysate or peripheral human neutrophils (PMN). DPI, a NOX inhibitor, was included as a positive control for NOX inhibition. ^b NO production was measured in the presence of 1–50 μM of test drugs. L-NAME (a nonselective NOS inhibitor) was included as a positive control. Data were calculated as 50% inhibitory concentration (IC₅₀) and expressed as the mean ± SEM from 3–6 experiments performed on different days using BV2 cell lysate or PMN from different passages or donors. NA: not active. “—”: samples not tested. ^c *P* < 0.05 as compared with relative positive control, respectively.

Camphoratin F (methyl 7β-hydroxy-3,11-dioxo-4α-methylergosta-8,24(28)-dien-26-oate, 6): colorless powder (MeOH); mp 100–101 °C; [α]_D²⁵ +174 (*c* 0.008, MeOH); UV (MeOH) λ_{max} (log ε) 251 (4.05) nm; IR (KBr) ν_{max} 3386, 2967, 2877, 1732, 1711, 1669, 1235, 1197, 1167, 1083 cm⁻¹; ¹H NMR and ¹³C NMR, see Tables 1 and 3; ESIMS *m/z* 507 [M + Na]⁺; HRESIMS *m/z* 507.3083 (calcd for C₃₀H₄₄O₅Na 507.3086).

Camphoratin G (7α-hydroxy-3,11-dioxo-4α-methylergosta-8,24(28)-dien-26-oic acid, 7): colorless powder (MeOH); mp 196–198 °C; [α]_D²⁵ +139 (*c* 0.007, MeOH); UV (MeOH) λ_{max} (log ε) 247 (4.33) nm; IR (KBr) ν_{max} 3420, 2964, 2930, 2875, 1707, 1659, 1171 cm⁻¹; ¹H NMR and ¹³C NMR, see Table 1 and 3; ESIMS *m/z* 493 [M + Na]⁺; HRESIMS *m/z* 493.2929 (calcd for C₂₉H₄₂O₅Na 493.2930).

Camphoratin H (4α-methylergosta-8,24(28)-diene-3,11-dione, 8): colorless syrup; [α]_D²⁵ +41 (*c* 0.008, MeOH); UV (MeOH) λ_{max} (log ε) 248 (3.94) nm; IR (KBr) ν_{max} 2965, 2940, 2877, 1711, 1678 cm⁻¹; ¹H NMR and ¹³C NMR, see Tables 1 and 3; ESIMS *m/z* 447 [M + Na]⁺; HRESIMS *m/z* 447.3237 (calcd for C₂₉H₄₄O₂Na 447.3239).

Camphoratin I [(25S)-26-hydroxyergosta-7,22-dien-3-one, 9]: colorless powder (MeOH); mp 192–193 °C; [α]_D²⁵ +128 (*c* 0.003, MeOH); IR (KBr) ν_{max} 3336, 2956, 2873, 1716, 1024 cm⁻¹; ¹H NMR and ¹³C NMR, see Tables 1 and 3; ESIMS *m/z* 435 [M + Na]⁺; HRESIMS *m/z* 435.3242 (calcd for C₂₈H₄₄O₂Na 435.3239).

Camphoratin J (methyl 3,11-dioxo-4α-methyl-14β-ergosta-8,24(28)-dien-26-oate, 10): colorless needles (MeOH); mp 100–102 °C; [α]_D²⁵ +164 (*c* 0.005, MeOH); UV (MeOH) λ_{max} (log ε) 250 (4.35) nm; IR (KBr) ν_{max} 2953, 2873, 2856, 1738, 1709, 1669, 1460, 1453, 1375, 1077 cm⁻¹; ¹H NMR and ¹³C NMR, see Tables 1 and 3; ESIMS *m/z* 491 [M + Na]⁺; HRESIMS *m/z* 491.3135 (calcd for C₃₀H₄₄O₄Na 491.3137).

Preparation of (R)-MTPA Ester of 9. To a solution of **9** (0.5 mg) in pyridine (0.4 mL) was added (*S*)-MTPA chloride (25 μL), and the mixture was allowed to stand for 3 h at room temperature. The reaction was quenched by the addition of 1.0 mL of H₂O, and the mixture was subsequently extracted with EtOAc (3 × 1.0 mL). The EtOAc-soluble layers were combined, dried over anhydrous MgSO₄, and evaporated. The residue was subjected to silica gel column chromatography using

n-hexane–EtOAc (4:1) as the eluent to yield the (*R*)-MTPA ester, **9a** (0.7 mg). Selective ¹H NMR (500 MHz, CDCl₃) of **9a**: δ 7.38–7.53 (5H, m, Ph), 5.21 (1H, dd, *J* = 15.0, 7.5 Hz, H-23), 5.16 (1H, dd, *J* = 15.0, 7.5 Hz, H-22), 4.17 (2H, br d, *J* = 6.4 Hz, H₂-26), 3.54 (3H, s, OMe), 1.02 (3H, d, *J* = 6.5 Hz, H₃-21), 1.01 (3H, s, H₃-19), 0.95 (3H, d, *J* = 7.0 Hz, H₃-28), 0.85 (3H, d, *J* = 7.0 Hz, H₃-27), 0.57 (3H, s, H₃-18).

In Vitro Cytotoxicity Assay. The KB-MDR cell line system was a generous gift from Professor Y.-C. Cheng, Yale University, and was developed using stepwise vincristine selection as reported.²³ The MDR cell line KB-VIN and the parent KB nasopharyngeal were propagated in RPMI-1640 medium supplemented with 25 mM HEPES, 10% fetal bovine serum, 100 U/mL penicillin G, 100 μg/mL streptomycin, and 250 ng/mL amphotericin B and cultured at 37 °C in a humidified atmosphere of 95% air/5% CO₂. KB-VIN cells were challenged with 0.5 μg/mL vincristine every two weeks, and drug was removed at least one day prior to using the cells. For the antiproliferation assay, trypsinized cells were seeded in 96-well microplates at densities of 5000 cells per well with compounds added from DMSO-diluted stock to give a dose range of 20 down to 0.16 μM. After 3 days in culture, attached cells were fixed in situ with 10% trichloroacetic acid and then stained with 0.4% sulforhodamine B in 1% HOAc.²⁴ The absorbance at 562 nm was measured using a microplate reader after solubilizing the bound dye. Results were plotted using Prism software (GraphPad, San Diego, CA). The mean EC₅₀ is the concentration of agent interpolated from graphical results that caused a 50% reduction in the cell number of treated versus untreated cells and is an average from at least two independent determinations; variation was less than 5% of the mean.

Microglial Cell Culture and Measurements of NO.²⁴ The murine microglial cell line (BV2) was cultured in Dulbecco's modified Eagle medium (Gibco, USA) supplemented with 5% fetal bovine serum (Hyclone). Production of NO was measured by the accumulation of nitrite in the culture medium 24 h after stimulation with LPS (0.5 μg/mL) by the Griess reagent. NO production was measured in the presence of 1–50 μM of test drugs. L-NAME (a nonselective NOS inhibitor) was included as a positive control. Data were calculated as 50% inhibitory concentration (IC₅₀) and expressed as the mean ± SEM from 3–6 experiments performed on different days.

Measurement of NOX Activity. Activity was measured as ROS production triggered with NADPH (200 μM) or fMLP (2 μM) in the presence of 1–50 μM of test drugs in BV2 cell lysate or PMN. DPI, a NOX inhibitor, was included as a positive control for NOX inhibition. Methodology was been previously described.²⁵

Measurement of DPPH Radical-Scavenging Capacity. DPPH radical-scavenging capacity assay was performed as in our previous report.¹⁹ Briefly, drugs were diluted in MeOH to a range of concentrations (10–50 μM). DPPH solution (200 μL; 200 μM in MeOH) was added to 10 μL of each diluted sample in a 96-well microplate, and the resulting solution was allowed to react for 30 min in the dark at ambient temperature. The absorbance caused by the DPPH radical at 517 nm was determined by a microplate-spectrophotometer. The radical-scavenging capacity was expressed as delta OD₅₁₇ (ΔOD₅₁₇), and values were the means of three replicates. Trolox, an antioxidant, was included as a reference.

Acknowledgment. The authors acknowledge Dr. Tun-Tschu Chang (Division of Forest Protection, Taiwan Forestry Research Institute, Taipei, Taiwan) for his identification and the financial support from the National Science Council, Taiwan, Republic of China, awarded to T.-S.W. This investigation is supported in part by Taiwan Department of Health Cancer Research Center of Excellence (DOH99-TD-C-111-005) awarded to T.-S.W. and also supported in part by grant CA-17625 from the National Cancer Institute, NIH, awarded to K.-H.L.

Supporting Information Available: ¹H and ¹³C NMR spectra of **1–10** are available free of charge via the Internet at <http://pubs.acs.org>.

References and Notes

- Wu, S. H.; Yu, Z. H.; Dai, Y. C.; Chen, C. T.; Su, C. H.; Chen, L. C.; Hsu, W. C.; Hwang, G. Y. *Fungal Sci.* **2004**, *19*, 109–116.
- Tsai, Z. T.; Liaw, S. L. *The Use and the Effect of Ganoderma*; Sang-Yun Press: Taichung, Taiwan, 1982; p 116.
- Shen, Y. C.; Wang, Y. H.; Chou, Y. C.; Chen, C. F.; Lin, L. C.; Chang, T. T.; Tien, J. H.; Chou, C. J. *Planta Med.* **2004**, *70*, 310–314.

- (4) Chen, C. H.; Yang, S. W.; Shen, Y. C. *J. Nat. Prod.* **1995**, *58*, 1655–1661.
- (5) Cherng, I. H.; Chiang, H. C.; Cheng, M. C.; Wang, Y. *J. Nat. Prod.* **1995**, *58*, 365–371.
- (6) Shen, C. C.; Kuo, Y. C.; Huang, R. L.; Lin, L. C.; Don, M. J.; Chang, T. T.; Chou, C. J. *J. Chin. Med.* **2003**, *14*, 247–258.
- (7) Cherng, I. W.; Wu, D. P.; Chiang, H. C. *Phytochemistry* **1996**, *41*, 263–267.
- (8) Shirane, N.; Takenaka, H.; Ueda, K.; Hashimoto, Y.; Katoh, K.; Ishii, H. *Phytochemistry* **1996**, *41*, 1301–1308.
- (9) Abraham, R. J.; Monasterios, J. R. *J. Chem. Soc., Perkin Trans. 2* **1974**, 662–665.
- (10) Wu, D. P.; Chiang, H. C. *J. Chin. Chem. Soc.* **1995**, *42*, 797–800.
- (11) Rösecke, J.; König, W. A. *Phytochemistry* **2000**, *54*, 757–762.
- (12) Hu, S. H.; Genain, G.; Azerad, R. *Steroids* **1995**, *60*, 337–352.
- (13) Rösecke, J.; König, W. A. *Phytochemistry* **2000**, *54*, 603–610.
- (14) D'Auria, M. V.; De Riccardis, F.; Minale, L.; Riccio, R. *J. Chem. Soc., Perkin Trans. 1* **1990**, 2889–2893.
- (15) Fu, X.; Ferreira, M. L. G.; Schmitz, F. J.; Kelly, M. *J. Org. Chem.* **1999**, *64*, 6706–6709.
- (16) Burgoyne, D. L.; Andersen, R. J.; Allen, T. M. *J. Org. Chem.* **1992**, *57*, 525–528.
- (17) Shoji, N.; Umeyama, A.; Shin, K.; Takeda, K.; Arihara, S.; Kobayashi, J.; Takei, M. *J. Org. Chem.* **1992**, *57*, 2996–2997.
- (18) Van den Worm, E.; Beukelman, C. J.; Van den Berg, A. J.; Kroes, B. H.; Labadie, R. P.; Van Dijk, H. *Eur. J. Pharmacol.* **2001**, *433*, 225–230.
- (19) Lin, L. C.; Wang, Y. H.; Hou, Y. C.; Chang, S.; Liou, K. T.; Chou, Y. C.; Wang, W. Y.; Shen, Y. C. *J. Pharm. Pharmacol.* **2006**, *58*, 129–135.
- (20) Liou, K. T.; Shen, Y. C.; Chen, C. F.; Tsao, C. M.; Tsai, S. K. *Eur. J. Pharmacol.* **2003**, *475*, 19–27.
- (21) Coussens, L. M.; Werb, Z. *Nature* **2002**, *420*, 860–867.
- (22) Peng, C. C.; Chen, K. C.; Peng, R. Y.; Chyau, C. C.; Su, C. H.; Hsieh-Li, H. M. *J. Ethnopharm.* **2007**, *109*, 93–103.
- (23) Ferguson, P. J.; Fisher, M. H.; Stephenson, J.; Li, D.-H.; Zhou, B.-S.; Cheng, Y.-C. *Cancer Res.* **1988**, *48*, 5956.
- (24) Rubinstein, L. V.; Shoemaker, R. H.; Paull, K. D.; Simon, R. M.; Tosini, S.; Skehan, P.; Scudiero, D. A.; Monks, A.; Boyd, M. R. *J. Nat. Cancer Inst.* **1990**, *82*, 1113.
- (25) Wang, Y. H.; Wang, W. Y.; Chang, C. C.; Liou, K. T.; Sung, Y. J.; Liao, J. F.; Chen, C. F.; Chang, S.; Hou, Y. C.; Chou, Y. C.; Shen, Y. C. *J. Biomed. Sci.* **2006**, *13*, 127–141.

NP1002143